γ rays from muon capture in I, Au, and Bi

David F. Measday,* Trevor J. Stocki,† and Heywood Tam‡
Department of Physics and Astronomy, University of British Columbia, Vancouver, British Columbia, Canada V6T 1Z1
(Received 5 December 2006; published 20 April 2007)

A significant improvement has been made in the identification of γ rays from muon capture in I, Au, and Bi, all monisotopic elements. The $(\mu^-, \nu n)$ reaction was clearly observed in all nuclei, but the levels excited do not correlate well with the spectroscopic factors from the $(d,{}^3\mathrm{He})$ reaction. Some $(\mu^-, \nu 2n)$, $(\mu^-, \nu 3n)$, $(\mu^-, \nu 4n)$, $(\mu^-, \nu 5n)$ and other reactions have been observed at a lower yield. The muonic x-ray cascades have also been studied in detail.

DOI: 10.1103/PhysRevC.75.045501 PACS number(s): 23.40.−s, 36.10.Dr, 27.60.+j, 27.80.+w

I. INTRODUCTION

We continued our study of muon capture in nuclei. Our earlier article described the results for capture on Ca, Fe, and Ni [1]. Muon capture in nuclei is a complex phenomenon that is far from understood, so we have extended our study to heavier elements for which very little information is available. We chose iodine, gold, and bismuth because they are composed of only one isotope each, and thus an isotopic target can be obtained economically in the quantity of 50 to 200 g, which is needed for such experiments.

The present situation with regard to muon capture has recently been reviewed by Measday [2]. We focus on the experiments that observe the γ rays following the muon capture, which occurs via the weak interactions from the muonic 1s level. Because the mass of the muon is about 106 MeV/c^2, there is plenty of energy available when the muon is absorbed on a proton in the nucleus, and, although the neutrino takes away most of the energy, the product nucleus can be excited to 10 or 20 MeV. In lighter elements the most important reactions are (μ^-, ν) and $(\mu^-, \nu n)$, with $(\mu^-, \nu 2n)$ being only about 5 to 10%, and proton emission can reach 10% or more. However, for heavy nuclides more neutrons are emitted thus, about 10% of the time the (μ^-, ν) reaction feeds bound states in the product having the same mass as the target nucleus, about 45% of the time a single neutron is given off, 25% of the time two neutrons are emitted, 10% of the time three neutrons are emitted, and 10% of the time four or more neutrons are emitted. More complex reactions emitting protons or αs do occur but are very rare, $<1\%$ in total for heavy elements. All of the reactions can lead to excited states, so quite a variety of γ rays can be produced. For heavy nuclei the Doppler broadening of these γs is not as important as in light nuclei, so the observed resolution is better than for light nuclei, but this is more than compensated by the vast number of levels in heavy nuclei, and thus the number of possible transitions runs into the hundreds.

Because the capture reactions occur up to a few hundred nanoseconds after the muon stop, the coincidence requirement is not very stringent in removing background from the experimental area, which is bathed in thermal neutrons, and 1 MeV neutrons are produced in the muon capture itself, and so add to the problems. Thus it is critical to measure the γ-ray energies with care and precision. A key advantage that we have is that the energies and branching ratios of γ rays are much better known now (and much more easily accessible from the National Nuclear Data Center). Modern γ-ray detectors are somewhat better than they used to be, but more important is that they are larger and more efficient for γ rays of a few MeV. Thus an experiment can now identify γ rays of 2 to 6 MeV, even though the yield may be fairly low. In addition a modern accelerator like TRIUMF has a macroscopic duty cycle of 100%, so the data can be taken at a higher rate. We have thus revisited muon capture on natural iodine, gold, and bismuth. The runs lasted 1 or 2 h each, and the data are dependable and rare transitions were observed. For iodine and gold we analyzed at least two runs independently, but for bismuth the spectra were summed.

Previous experiments are sparse. Backenstoss *et al.* [3] studied muon capture on six elements including ^{127}I and ^{209}Bi. They identified eight lines in iodine, and seven lines in bismuth. Evans [4] studied nine elements, including ^{197}Au, and specified seven lines. In general we are in excellent agreement with these earlier observations, although a few minor discrepancies exist.

For the (μ^-, ν) reaction, there are no useful (n, p) or $(d,{}^2\mathrm{He})$ data to compare with, and calculations for heavy elements are too difficult to undertake. For the $(\mu^-, \nu n)$ reaction, it has been found in lighter nuclei that the closest comparison is to the (γ, p) reaction; unfortunately for our targets, there are data for only bismuth [5], and the Coulomb effects for such a heavy nucleus overpower any similarity. Comparison with the $(d,{}^3\mathrm{He})$ reaction is useful, but the correlations are not that close; there are measurements for iodine [6,7], gold [8–10], and bismuth [11,12]. We compare our results with those data.

For heavy elements, the muonic x rays are complex, and many series are observed. Our spectra contain both capture γ rays and muonic x rays, and both have to be analyzed in parallel. Because of the interest in nuclear radii the energies of the muonic x rays have been well studied, and we can use these energies as calibrations; the shapes from the figures

*Electronic address: measday@phas.ubc.ca
†Present address: Radiation Protection Bureau, Ottawa, Ontario, Canada K1A 1C1.
‡Present address: California Institute of Technology, Pasadena, CA 91125, USA.

 ©2007 The American Physical Society

are also helpful. For iodine, Klein [13] has obtained accurate energies in his diploma thesis, but fortunately the numbers are reproduced in the compendium of Fricke [14]. Because of the complex shape of the x rays due to the hyperfine interaction, the older article of Lee *et al*. [15] was actually more useful, especially as they gave energies for the $(3d\text{-}2p)$ and $(4f\text{-}3d)$ muonic x rays. These energies are also given in the older, but still useful, compendium of Engfer *et al*. [16]. For gold there is a quite complete study of the x-ray energies and hyperfine effects by Powers *et al*. [17]. Again this work is very useful for calibration and for shape analysis. Fricke *et al*. [14] quote another thesis [18], but this is not much use because of the structure. For bismuth there is the study of the energies and hyperfine effects by Bardin *et al*. [19], and of Powers [20]; we used these results for energy calibrations.

The x-ray intensities are used as a normalization for the capture γ rays. Thus it is necessary to understand the cascade in detail. The only previous work to study heavy elements was that of Hartmann *et al*. [21], who studied Mg, Al, In, Ho, and Au in great detail, more than we actually need. For iodine and bismuth, we thus needed to study the cascades in our own data, and gold was a useful check.

In heavy elements other effects complicate the de-excitation of the muonic atom. First for elements where the muonic transitions have more energy than the neutron separation energy (8.07 MeV in Au and 7.46 MeV in Bi), it is possible to have radiationless transitions akin to the (γ, n) reaction, thus a prompt neutron is emitted and the muon is left in a $1s$ state around a ^{196}Au or ^{208}Bi nucleus. It is not relevant for iodine, for which the neutron binding (9.14 MeV) is too high. We estimate that the probability for this effect is $5 \pm 5\%$ in Au and $7 \pm 2\%$ in Bi [22,23]. In bismuth, this takes place instead of a (3-1) transition. Thus muon capture actually occurs in some instances from the lighter isotope, but the distribution of levels excited will be similar, though not identical, to that of the target nucleus. Also there is the possibility of detecting γ rays from a ^{196}Au or ^{208}Bi nucleus from this effect.

A further complication is that in bismuth, some nuclear levels are excited during the cascade, and these levels de-excite with the muon still in place, thus the Coulomb effect displaces the γ-ray energy by a few keV, the so-called isomer shift. This occurs about 8.5% of the time and probably reduces the intensity of the $(3d\text{-}2p)$ muonic transition accordingly [24–26]. We have included this effect in the accounting of the cascade intensity. This effect might also occur in gold.

Because there are several x-ray series observed, we can estimate the absolute intensity of the final transition in the series and use this as a check on the efficiency of the germanium detector. We find that this is the best way to estimate the self-absorption in the target at low energies (<500 keV).

II. EXPERIMENT

These data were taken at the same time as our previous data for ^{14}N [27], and for Ca, Fe, and Ni [1], so we simply outline the technique. The experiment was performed on beamline M9B at TRIUMF. The beamline includes a 6 m, 1.2 T superconducting solenoid in which a 90 MeV/$c\,\pi^-$ beam decays into muons. The resulting backward μ^- are then separated from the pions by a bending magnet and pass through a collimator into the experimental area, illustrated in Fig. 1. The collimator was made of lead but lined with polyethylene to reduce the number of neutrons and γ rays from muons stopping in the collimator. The beam rate was about 2×10^5 s^{-1}, with negligible pions but with ~20% electrons. The muon beam is somewhat diffuse, so a muon stopping in the target is selected by three plastic scintillators, two before and one large one in anticoincidence after the target. The defining counter, just before the target was 51 mm in diameter. The counters were wrapped in aluminum foil with black electrical tape, which is made of polyvinyl chloride (PVC). Many muons stop in the defining counter, mainly in the carbon but some in aluminum and also in chlorine. The iodine target was made of crystals with a mass of 170 g; it was 10 mm thick or 2.7 g/cm^2. The gold target was a disk, 48 mm in diameter, and had a mass of 32.75 g; it was 0.95 mm thick or 1.8 g/cm^2. The bismuth target was a powder, 9 cm in diameter, and had a mass of 221 g; it was 10 mm thick or 3.5 g/cm^2. For some runs a mu-metal shield was used to reduce the magnetic field at the target, but it produced a noticeable nickel background. Fortunately, these γ rays have been identified in our previous study [1].

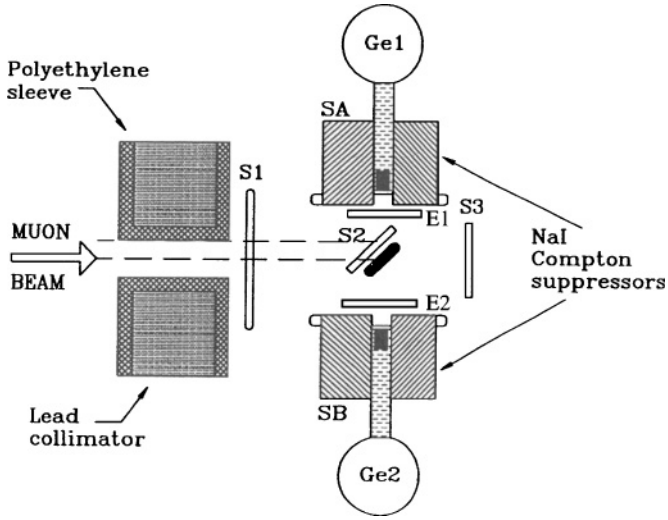

FIG. 1. Experimental setup. Only the spectra from the larger HPGe detector were analyzed.

There were always two HPGe γ-ray detectors at right angles to the beam line, but only the larger detector was used in the analysis. The gold target was used first, immediately after the nitrogen experiment [27] and "our own" detector was in place. This n-type detector has an efficiency of 44% with respect to a 7.62-cm diameter by 7.62 cm long Na(Tl) detector. It has a timing resolution of about 6 ns and an in-beam resolution of 2.6 keV at 1.3 MeV, 4 keV at 2.2 MeV, and about 9 keV at 6.1 MeV. For the iodine and bismuth targets, the main detector was replaced with what is called locally the Toronto detector; it is a p-type detector and has an efficiency of 37.5%. It has a timing resolution of about 7 ns, and a similar in-beam resolution of 3 keV at 1.3 MeV, 5 keV at 2.8 MeV, and 10 keV at 6.1 MeV. Both detectors had NaI(Tl) Compton suppression

anticoincidence shields, but these were not used. They can introduce efficiency concerns for cascading transitions. In front of all the HPGe detectors, there was a plastic scintillator to tag electrons entering the detector. The electronics consisted of standard spectroscopic amplifiers and timing filter amplifiers, followed by constant fraction discriminators. The event trigger was a HPGe pulse above a hardware discriminator at typically 100 keV. The closest muon was selected from a delayed signal from the plastic defining scintillators. Information recorded for each event included the pulse heights in the two HPGe detectors and the defining plastic scintillator, as well as timing information. Each event was read by a starburst and a VAXstation 3200 and written to tape. Over 100 online histograms were kept for every target to monitor the progress of the experiment. The cuts could be reanalyzed offline, but the histograms had been well chosen, and this was rarely done. For analysis of the γ-ray spectra, we chose the total histogram, so x rays and γ rays were together, thus improving the energy calibration and efficiency measurements. If there was overlap, the events in coincidence with the muon stop could be selected to give a purer x-ray spectrum. Because the muon capture is very fast, typically within 100 ns, the x-ray spectrum normally had significant γ-ray content anyway and vice-versa.

TABLE I. γ-ray and muonic x-ray energies used for calibration, taken from Measday [2], NNDC [28], Lee *et al.* [15], Helmer and van der Leun [29], Dewey *et al.* [30], Raman [31], and Revay [32].

Line	Energy(error) in keV	Reference
μ-mesic O($2p$-$1s$)	133.535(2)	[2]
^{196}Pt	355.684(2)	[28]
μ-mesic I($4f$-$3d$)	388.16(20)	[15]
Annihilation	510.9912(14)[a]	[2]
^{208}Pb	583.191(2)	[28]
^{124}Te	645.855(2)	[28]
^{126}Te	666.352(10)	[28]
^{56}Fe(n, n')	846.771(5)	[28]
μ-mesic I($3d_{3/2}$-$2p_{1/2}$)	1150.42(15)	[15]
^{60}Co	1173.228(3)	[29]
^{41}Ar	1293.586(7)	[28]
^{60}Co	1332.492(4)	[29]
$np \rightarrow \gamma d$	2223.2484(4)	[30]
^{208}Pb	2614.533(13)	[28]
^{16}N	6129.14(3)	[2]
^{56}Fe(n, γ)	7645.55(3)	[31]
	7645.49(9)	[32]

[a]This energy is 7.7(14) eV below the mass of the electron [33].

III. DATA ANALYSIS

The identification of a γ ray is via its energy only. The stability of the amplifiers was quite remarkable and the gain changed by less than 1 channel in 1000 over several days. The main effect seemed to be a slight pedestal shift. We took the energy calibration from each spectrum itself and rarely used neighboring runs, though sometimes this was necessary for calibrations at a few MeV. For the calibration a quadratic form was taken, and the histogram was divided into sections. The spectra consisted of 2048 channels, and for our medium gain spectrum at 1.3 keV per channel, the sections would be 100–700, 700–1300, 1300–2000, and 2000–2700 keV. For the low gain spectrum at 5.3 keV per channel, the sections were typically 100–1400, 1400–2200, and 2200–10850 keV. Only the highest energy section was used to define yields; below 2.5 MeV, the yields were taken from the medium gain spectrum. The energy calibration was good to about 0.1 keV up to 1.5 MeV, but deteriorated rapidly above this. For bismuth, the 2615-keV line from ^{208}Pb is a superb beacon, but for gold and iodine, it was necessary to use the muonic x rays. The thermal neutron (n, γ) lines were not as noticeable for these heavy elements, because the timing gate was reduced from that used for the lighter elements. This meant a smaller background, but also made it difficult to calibrate the energy. Fortunately this is not critical because the only muon capture γ rays found above 3 MeV were in bismuth, for which the calibration was more secure. Typical calibration lines are given in Table I. They are known better than could be utilized in this experiment. Note that the energy given here is the γ-ray energy, not the transition energy, which can be a little higher because of the recoil correction.

Many levels, which are excited in muon capture, have two or more de-exciting transitions. If we have a marginal observation of a single γ ray, we normally do not mention it, but if we have a marginal identification of two, or even better three, transitions, then we consider this more dependable evidence.

The relative efficiency of the two detectors was obtained with a ^{152}Eu source for which the intensities are well known between 122 and 1408 keV [28,34]. However, for heavy elements the self-absorption is more serious than for our previous publication, thus we have used the muonic x rays at low energy to obtain the effective efficiency, because the source of the x rays and γ rays is distributed in the target identically. Thus our technique was to take a muonic x ray around 1 MeV as the normalizing transition and to use lower energy x rays for obtaining the effective efficiency, which departed from the ^{152}Eu results below about 600 keV; the absorption was quite severe below 200 keV; see Fig. 2. For the higher energies we obtained the energy dependence of the efficiency by using

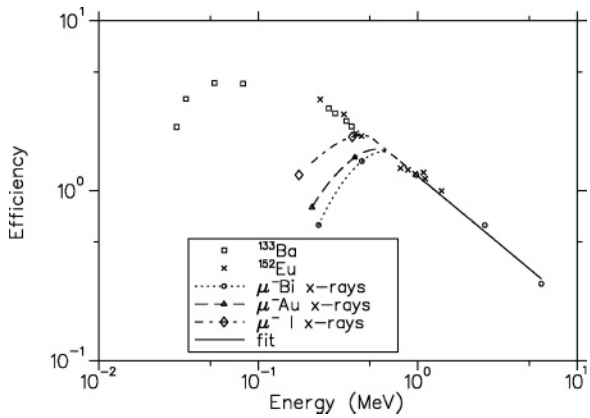

FIG. 2. The effective efficiency curves for the iodine, gold, and bismuth targets, including the self-absorption effect.

TABLE II. The muonic Lyman (or K) series for iodine, giving the observed energy and the absolute intensity per muon stop, normalized to 100% for the sum of this series.

μ x ray	Energy (keV)	Intensity (%)
$2p_{1/2}$-$1s_{1/2}$	3667.36(4)[a]	43.9(20)
$2p_{3/2}$-$1s_{1/2}$	3723.74(3)[a]	47.9(20)
$3p_{1/2}$-$1s_{1/2}$	4809(3)	
$3p_{3/2}$-$1s_{1/2}$	4824(3)	Sum = 5.3(13)
$4p$-$1s$	5209(3)	1.5(5)
$5p$-$1s$	5389(3)	0.6(4)
$6p$-$1s$	5486(5)	0.5(4)
$7p$-$1s$	5550(10)	0.3(3)

[a]These energies are used as calibrations [14].

the bismuth muonic x rays for the Toronto detector, i.e., for the bismuth and iodine targets, and the gold muonic x rays for "our detector"; as a check, a short run of iodine was also taken with "our detector", and this confirmed that at the higher energies the detectors had very similar efficiencies. At lower energies the effective efficiency was smaller as the Z of the target increased.

Above 900 keV for the Toronto detector, we used the standard form of:

$$\ln(\text{eff}) = 0.200 - 0.780 \ln \text{E}_\gamma \tag{1}$$

and for "our detector" we used:

$$\ln(\text{eff}) = 0.200 - 0.786 \ln \text{E}_\gamma . \tag{2}$$

Note that this value for the Toronto detector is slightly different from our previous publication because we have reanalyzed the data for the cascade of the bismuth muonic x rays, which define the high energy efficiency. It affects only the γ rays above 2 MeV and would not make a significant difference to our results for Ca, Fe, or Ni [1].

IV. RESULTS FOR IODINE

We shall first discuss the muonic x-ray cascades. These results are used in determining the effective detector efficiency,

TABLE III. The muonic Balmer (or L) series for iodine, giving the observed energy and the absolute intensity per muon stop, normalized to 91.8% from the $(2p$-$1s)$ transition.

μ x ray	Energy (keV)	Intensity (%)
$3d_{5/2}$-$2d_{3/2}$	1101.84[a]	56.8(20)
$3d_{3/2}$-$2d_{1/2}$	1150.42[b]	26.5(10)
$4d_{5/2}$-$2d_{3/2}$	1478–1496	4.2(10)
$4d_{3/2}$-$2d_{1/2}$	1541.4(10)	2.2(5)
$5d_{5/2}$-$2d_{3/2}$	1653–1676	1.2(5)
$5d_{3/2}$-$2d_{1/2}$	1720(5)	0.6(4)
$6d_{5/2}$-$2d_{3/2}$	~1764	0.2(2)
$6d_{3/2}$-$2d_{1/2}$	1820(3)	0.1(1)

[a]See Ref. [35].
[b]This energy is used as a calibration [15].

TABLE IV. The muonic Paschen (or M) series for iodine, giving the observed energy and absolute intensity per stop, normalized to a total of 88.6%.

μ x ray	Energy (keV)	Intensity (%)
$4f_{7/2}$-$3d_{5/2}$	388.16(20)[a]	42.7(20)
$4f_{5/2}$-$3d_{3/2}$	394.2(2)	28.4(15)
$5f_{7/2}$-$3d_{5/2}$	566.6(2)	5.6(10)
$5f_{5/2}$-$3d_{3/2}$	573.7(2)	3.7(5)
$6f_{7/2}$-$3d_{5/2}$	663.5[b]	3.5[c]
$6f_{5/2}$-$3d_{3/2}$	670.2[b]	2.2[c]
$7f_{7/2}$-$3d_{5/2}$	722.5(3)	1.2(6)
$7f_{5/2}$-$3d_{3/2}$	729.7(3)	0.6(4)
$8f_{7/2}$-$3d_{5/2}$	785[b]	0.4(2)
$8f_{5/2}$-$3d_{3/2}$	792[b]	0.3(2)

[a]Calibration from Ref. [15].
[b]Difficult to distinguish from the strong 666-keV line in ^{126}Te; energy from adjusting the point nucleus value.
[c]Estimate from intensity pattern.

and in the overall normalization of the muon capture γ rays; however, they are also interesting in their own right. Note that for iodine, we work by first normalizing the Lyman series $(np$-$1s)$ to 100%, and then the Balmer series $(nd$-$2p)$ is normalized to the $(2p$-$1s)$ transition, the Paschen series (4-3) is normalized to the sum of the $(3d$-$2p)$ and $(3p$-$1s)$ lines, and the Brackett series is normalized to the sum of the $(4f$-$3d)$, $(4d$-$2p)$ and $(4p$-$1s)$ lines, etc. Our data are not sufficiently accurate to justify a more sophisticated analysis, which would include $E2$ transitions, etc. These have been included in experiments and calculations addressing the cascade specifically, but they are very small corrections. Note that for gold and bismuth, the cascade is more complex, with other terms needed.

Our results for the Lyman series for iodine are given in Table II.

Our results for the Balmer series are given in Table III. Note that the $(3d$-$2p)$ transition is the one used for the overall normalization of the iodine spectra.

The Paschen series and Brackett series for muonic iodine are presented in Tables IV and V, respectively. These are used to obtain the effective efficiency of the HPGe detector.

TABLE V. The muonic Brackett (or N) series for iodine, giving the observed energy and absolute intensity per stop, normalized to a total of 79.5%.

μ x ray	Energy (keV)	Intensity (%)
$5g$-$4f$	179.4(2)	62.9(20)
$6g$-$4f$	276.3(2)	8.9(10)
$7g$-$4f$	334.9(3)	4.1(8)
$8g$-$4f$	372.4(2)	2.0(4)
$9g$-$4f$	398.4[a]	1.1[b]
$10g$-$4f$	417.0[a]	0.5[b]

[a]Difficult to distinguish; energy from adjusting the point nucleus value.
[b]Estimate from intensity pattern.

TABLE VI. Values of the experimental parameters for muon capture in iodine, gold, and bismuth [36,37].

Quantity	Iodine	Gold	Bismuth
Muonic lifetime (ns)	85.6(22)	69.96(20)	73.5(4)
Muonic capture rate (s^{-1})	$11,270(300) \times 10^3$	$13,907(40) \times 10^3$	$13,232(70) \times 10^3$
Decay rate (s^{-1})	414×10^3	387×10^3	382×10^3
Capture probability (%)	96.45(9)	97.29(1)	97.19(2)
Target material	Crystals	Solid	Powder
Counts for ($3d$-$2p$) x rays	30,000	7,000	30,000

Note that we obtain 71.1(25)% for the yield of the muonic ($4f$-$3d$) transition, whereas Backenstoss *et al*. used 61% for their normalization. (Ours was via the ($3d$-$2p$) transition.) We have not applied a renormalization correction to the results of Backenstoss *et al*. (it would be ~17%), because their yields already seem slightly higher than ours, and furthermore, the total yield of muon captures would exceed 100%.

We now turn to the results for the muon capture γ rays. First we give in Table VI the values of the capture parameters used in our normalizations.

First we select the reaction ^{127}I(μ^-, $\nu\gamma$)^{127}Te. In previous experiments, the (μ^-, $\nu\gamma$) reaction has not been observed for nuclei heavier than calcium. Iodine seems to be an exception to this rule and we have quite convincing identifications for severals transitions; see Table VII. Note that neutrons are bound up to 6.29 MeV in ^{127}Te, yet the NNDC compendium does not list transitions for levels above 1.4 MeV.

The only level that we know is affected by cascading is that at 473 keV, which receives 1.0(5)% from the 1290-keV level, i.e., about 2/3 of the 1.4% production of the 473-keV level.

As is normal, many more γ rays are observed from the reaction ^{127}I(μ^-, $\nu n\gamma$)^{126}Te; see Table VIII. We illustrate the quality of our data in Fig. 3, showing a cluster of prominent lines between 550 and 760 keV. All these capture γ rays were reported by Backenstoss *et al*., except for the one at 652 keV in ^{126}Te, which has a yield of 1.9(4)%. In addition to the γ rays listed in Table VIII, we have also observed weak evidence for transitions from the levels at 2679, 2682, 2704, 2783, 2813, and 2834 keV at a yield of about 0.5%, but the uncertainty is significant (~50:50); note that ^{126}Te is bound up to 9.1 MeV, so many other transitions are energetically possible. The agreement with the earlier data of Backenstoss *et al*. [3] is good, but we observe many more transitions.

In Table IX, we present our results for the direct transitions to the levels by taking into account the known cascading; note that the cascading is always a lower limit as more transitions to these levels can come from weaker γ rays that are not confidently observed. With that proviso, we can then compare with other reactions such as ^{127}I(d,^{3}He)^{126}Te [7], using their Table III. Experience indicates that there is only a weak agreement with this reaction, and that proves to be true for this case, too, although our uncertainties are magnified because of the substantial cascading. Agreement with ^{127}I(γ, p)^{126}Te would normally be better, but there is no measurement.

In Table X we now present our data for the reaction ^{127}I(μ^-, $\nu 2n\gamma$)^{125}Te, which is quite strong, and the direct excitations are given in Table XI.

In Table XII we present our results for the reaction ^{127}I(μ^-, $\nu 3n\gamma$)^{124}Te, and in Table XIII our results for the direct excitation of the levels in ^{124}Te, taking into account the branching ratios, with the known cascading subtracted from the measurements of the γ-ray yields.

We have also observed γ rays from the $4n$, $5n$, and $6n$ reactions; see Table XIV. Such reactions are not observed in light elements. Note that for the reaction ^{127}I(μ^-, $\nu 4n\gamma$)^{123}Te, Backenstoss *et al*. listed two γ rays at 320 and 430 keV that we do not include in Table XIV; neither are attributed to ^{123}Te in modern compilations. They are not even listed in the decay products of ^{123}I in a 1970 compendium [38], so we do not understand the history of these identifications. Anyway Backenstoss *et al*. did not observe a γ ray at 320 keV, and neither do we. The γ ray at 430 keV is more interesting as

TABLE VII. Observed γ ray yields, per muon capture, for the reaction ^{127}I(μ^-, $\nu\gamma$)^{127}Te.

Level in ^{127}Te (keV)	J^π	Transition branching ratio (%)	Transition energy (keV)	Observed γ-ray yield (%)
340.6	$9/2^-$	100	252.4	3.4(4)
473.27	$5/2^+$	87	473.0(4)	1.4(4)
631.5	$7/2^-$	41	290.8	0.2(2)
		59	543.3	0.3(2)
685.5	$7/2^+$	100	685.7	0.4(4)
763.7	$(3/2^+,5/2^+)$	100	763.7	0.2(2)
783.4	$5/2^+$	84	783.7	1.0(4)
1290.3	$(5/2^+)$	52	817.0(6)	1.0(5)
		48	1290.3(8)	<1.0

TABLE VIII. Observed γ-ray yields, per muon capture, for the reaction ^{127}I(μ^-, $\nu n\gamma$)^{126}Te, compared to the previous results from Backenstoss *et al*. [3].

Level in ^{126}Te (keV)	J^π	Transition branching ratio (%)	Transition energy (keV)	Observed γ ray yield (%)	Previous results Ref. [3] (%)
666.35	2^+	100	666.33	42(3)	53(5)
1361.40	4^+	100	695.03	21(2)	20(3)
1420.18	2^+	93	753.82	6.4(5)	7.4(1.5)
1776.19	6^+	100	414.7	4.8(9)	
1873.40	0^+	100	1207.04	1.0(3)	
2013.17	4^+	58	651.79	1.9(4)	
		42	1346.79	1.2(4)	
2045.15	2	30	1378.76	0.5(5)	
		61	2045.17	1.0(5)	
2113.57		100	1447.21	<0.4	
2128.39	3^+	56	708.21	1.2(3)	
		20	766.98	0.3(2)	
		24	1462.03	0.3(3)	
2181.52	1	81	1515.15	1.5(3)	
2184.35	2^+	100	1517.99	1.0(3)	
2218.20	5^-	98	856.80	3.1(6)	
2309.19	4^+	21	889.03	1.0(5)[a]	
		79	947.78	0.5(5)	
2385.81		93	1719.45	1.6(4)	
2396.42		44	620.20	0.5(5)	
		56	1035.07	0.8(5)	
2421.15		31	999.66	0.3(3)	
		66	1754.78	1.1(5)	
2479.73		65	1118.33	0.3(1)	
		35	1813.37	0.5(3)	
2496.83		96	720.64	0.4(2)	
2503.55		83	1837.19	0.8(4)	
2515.21		90	297.01[b]	0.6(3)	
2533		100	1172.45	0.8(4)	
2585.46		90	1919.09	1.4(4)	
2661.43		81	1300.02	0.6(4)	
2765.75		100	989.57	1.0(3)	
2803.02		63	1382.82	0.5(2)	
		37	1441.70	0.6(2)	

[a]Probably contaminated; energy off.
[b]Calculated from energy levels; NNDC has 296.5(3) keV.

Backenstoss *et al*. observed a line at 431.3(5) keV, with a yield of 0.9(3)%, and we also observe a γ ray at exactly the same energy, viz. 431.3(5) keV, albeit with a slightly lower yield of 0.45(30)%, but we have no identification.

We have searched for γ rays from ^{120}Te, ^{119}Te, as well as from ^{126}Sb ^{125}Sb, ^{124}Sb (from proton producing reactions) and ^{123}Sn, ^{122}Sn (from α-producing reactions), but no evidence was found, with limits in the range of 0.5 to 1.0% yield. This is consistent with the activation results of Wyttenbach *et al*. [39], which indicate a total yield for iodine (including the ground state) of 0.04% for the (μ^-, νp) reaction, 0.3% for the (μ^-, νpn) reaction, 0.2% for the (μ^-, $\nu p2n$) reaction, and ~0.01% for the (μ^-, $\nu p3n$) reaction.

We can now summarize our results in Table XV for muon capture in iodine, giving our results, estimates for the

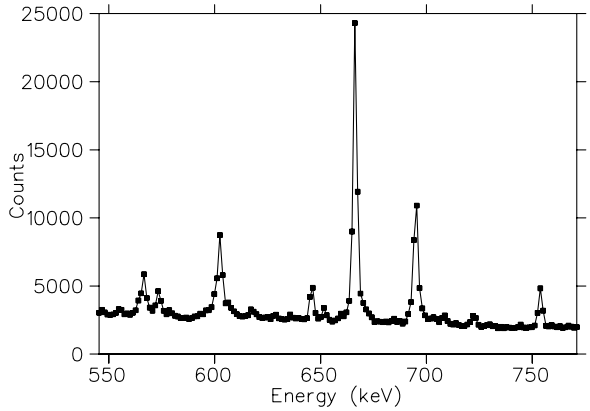

FIG. 3. A γ-ray spectrum for muon capture in iodine to illustrate the quality of our data. The iodine (5-3) muonic x rays are at 567 and 574 keV, at 603 and 646 keV are γ rays from ^{124}Te, and at 652, 666, 695, and 754 keV are γ rays from ^{126}Te. The iodine (6-3) x rays are partially obscured at 663 and 670 keV, and the (7-3) x rays are just visible at 722 and 729 keV.

TABLE IX. Our results for the direct excitation of a level in the reaction ^{127}I(μ^-, νn)^{126}Te, taking into account the known cascading, compared to the results from the reaction ^{127}I(d, ^{3}He)^{126}Te, at 27 MeV and 30° [7].

Level in ^{126}Te (keV)	Known cascading (%)	Direct yield per capture (%)	Yield in the reaction ^{127}I(d, ^{3}He)^{126}Te
0	44(3)	10(10)[a]	100
666.35	38.2(23)	4(3)	36
1361.40	13.9(15)	7.1(25)	1.8
1420.18	2.6(4)	4.3(7)	3.5
1776.19	2.1(6)	2.7(11)	5.7
1873.40	–	1.0(3)	2.0
2013.17	0.1(1)	3.0(6)	0.8
2045.15	–	1.6(8)	4.4
2113.57	–	<0.4	0.9
2128.39	–	2.0(5)	0.5
2181.52	–	1.9(4)	Sum
2184.35	–	1.0(3)	Is 4.3
2218.20	0.6(3)	2.5(7)	1.3
2309.19	–	0.6(6)	–
2385.81	–	1.7(4)	Sum
2396.42	–	1.3(10)	Is 3.4
2421.15	–	1.5(7)	–
2479.73	–	0.7(4)	–
2496.83	–	0.4(2)	–
2503.55	–	1.0(5)	–
2515.21	–	0.7(4)	–
2533	–	0.8(4)	–
2585.46	–	1.6(5)	1.4
2661.43	–	0.7(5)	1.5[b]
2765.75	–	1.0(3)	–
2803.02	–	1.1(3)	0.4[c]

[a]Estimate using the (d, ^{3}He) reaction.
[b]Energy given as 2653 keV.
[c]Energy given as 2794 keV.

TABLE X. Observed γ-ray yields, per muon capture, for the reaction ^{127}I(μ^-, $\nu 2n\gamma$)^{125}Te, compared to the previous results from Backenstoss *et al.* [3].

Level in ^{125}Te (keV)	J^π	Transition branching ratio (%)	Transition energy (keV)	Observed γ-ray yield (%)	Previous results Ref. [3] (%)
321.09	$9/2^-$	100	176.31	3(3)	Weak
443.56	$3/2^+$	38	408.07	0.8(3)	
		62	443.56	2.1(8)	
463.37	$5/2^+$	74	427.87	2.4(4)	1.7(5)
		26	463.37	0.9(3)	
525.23	$7/2^-$	82	380.45	1.6(4)	
636.09	$7/2^+$	99	600.60	1.6(10)	
642.21	$7/2^+$	87	606.71	1.3(8)	
671.44	$5/2^+$	84	635.95	0.9(4)	
786.61	$7/2^-$	93	465.55	1.0(5)	

ground-state transitions, and estimates for the yield of the missing transitions, using the results of MacDonald *et al.* [40], as analyzed by Measday [2], as a guide for the total neutron yields, but using systematic trends, rather than the actual measurements, and, finally, the calculations of Lifschitz and Singer [41] for the higher multiplicity modes.

V. RESULTS FOR GOLD

As indicated before, the gold runs were taken with "our detector," so a separate efficiency curve was needed. We used ^{152}Eu for the range 122 to 1408 keV, but used the gold muonic x rays for the extension to higher energies. Applying the same technique that we found useful for the other detector, we used the lower energy muonic x rays to define the self-absorption in the gold target. The gold target was a disk 0.95 mm in thickness (1.8 g/cm^2), so below 500 keV the effective efficiency fell off, and below 200 keV was too low to be useful.

We thus analyzed the muonic x rays with care. Fortunately for gold there are the measurements of Hartmann *et al.* to compare with Ref. [21]. The normalization followed the normal rule that the number of transitions entering a level must equal the number leaving. The situation is a bit more complex than for iodine in that there can be radiationless transitions that generate the ^{197}Au(γ, n) reaction, where the "γ" is a virtual muonic x ray. For bismuth this effect is known to occur with a probability of $7 \pm 2\%$ per stop [22]. For gold we have only a comment in the article of Powers *et al.* [17], without supporting evidence, that this effect "could be as large as 10%." We model this to mean that $5 \pm 5\%$ radiationless transitions occur from the $n = 3$ level. Thus we work by first normalizing the Lyman series (np-$1s$) to 95%, and then the Balmer series (nd-$2p$) is normalized to the ($2p$-$1s$) transition, the Paschen series (4-3) is normalized to the sum of the ($3d$-$2p$) and ($3p$-$1s$) lines, but adding back the 5%, and the Brackett series is normalized to the sum of the ($4f$-$3d$), ($4d$-$2p$) and ($4p$-$1s$) lines, etc. Note that Hartmann *et al.* did not include the radiationless transitions in their calculations. However, we

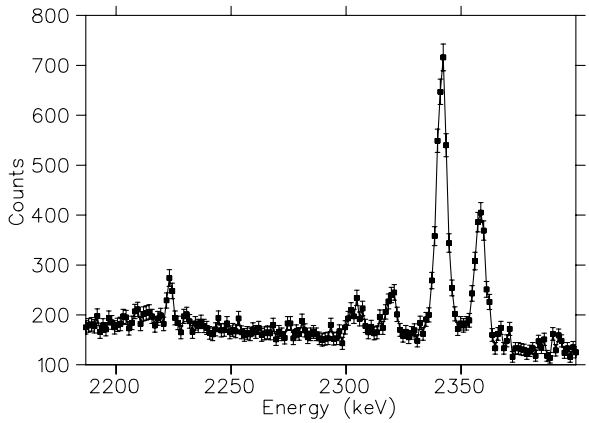

FIG. 4. A spectrum from gold, illustrating the complexity of the ($3d_{5/2}$-$2p_{3/2}$) muonic x rays at 2319, 2341, and 2358 keV; the triplet at 2305 keV is the ($3d_{3/2}$-$2p_{3/2}$) group. The ($3d_{3/2}$-$2p_{1/2}$) x ray is much higher at 2478 keV. The clear line at 2223.25 keV is a background from thermal neutron capture on hydrogen, viz. ($n + p \rightarrow \gamma + d$), and is a useful energy calibration.

TABLE XI. Our results for the direct excitation of a level in the reaction ^{127}I(μ^-, $\nu 2n$)^{125}Te, taking into account the known cascading.

Level in ^{125}Te (keV)	Known cascading (%)	Direct yield per capture (%)
321.09	1.4(5)	1.6(30)
443.56	–	2.9(9)
463.37	–	3.3(5)
525.23	–	2.0(5)
636.09	–	1.6(10)
642.21	–	1.5(8)
671.44	–	1.1(4)
786.61	–	1.1(5)

TABLE XII. Observed γ-ray yields, per muon capture, for the reaction ^{127}I(μ^-, $\nu 3n\gamma$)^{124}Te, compared to the previous results from Backenstoss *et al.* [3].

Level in ^{124}Te (keV)	J^π	Transition branching ratio (%)	Transition energy (keV)	Observed γ-ray yield (%)	Previous results Ref. [3] (%)
602.73	2^+	100	602.73	14.9(16)	15.6(15)
1248.59	4^+	100	645.86	4.7(4)	4.6(7)
1325.52	2^+	87	722.79	0.6(4)	2.8(8)
1746.97	6^+	100	498.38	1.34(30)	
1957.90	4^+	53	709.30	0.4(2)	
		42	1355.18	0.5(3)	
2039.30	2^+	53	713.78	0.3(2)	
		18	790.71	<0.3	
		28	1436.56	<0.6	
2091.62	2^+	98	1488.88	1.3(8)	

TABLE XIII. Our results for the direct excitation of a level in the reaction ^{127}I(μ^-, $\nu 3n$)^{124}Te, taking into account the known cascading.

Level in ^{124}Te (keV)	Known cascading (%)	Direct yield per capture (%)
602.73	7.1(10)	7.8(19)
1248.59	1.9(4)	2.8(6)
1325.52	0.3(2)	0.4(5)
1746.97	–	1.3(3)
1957.90	–	0.9(4)
2039.30	–	0.6(4)
2091.62	–	1.3(8)

are quoting their "experimental" results, which are not clearly explained, but they seem to use the cascade calculations to normalize the higher series and to use the efficiency from other targets to obtain absolute intensities for the Lyman and Balmer series. The Lyman and Balmer series in gold are given in Table XVI. The agreement with Hartmann *et al*. is satisfactory. In Fig. 4 we illustrate the complexity of the muonic x rays; this group is mainly from ($3d_{5/2}$-$2p_{3/2}$), except for the complex at 2305 keV, which is ($3d_{3/2}$-$2p_{3/2}$). The ($3d_{3/2}$-$2p_{1/2}$) x ray is much higher at 2478 keV. The clear line at 2223.25 keV is a background from thermal neutron capture on hydrogen, viz. ($n + p \rightarrow \gamma + d$) and is a useful energy calibration.

In Table XVII we present the muonic Paschen (or M) and Brackett (or N) series for gold. We compare with the experimental results of Hartmann *et al*. [21]. For these higher transitions, we have added back the 5% radiationless effect and so the values should be comparable. This is true for the Brackett series, but for the Paschen series there is a slight discrepancy. This is unfortunate, because it is the ($4f$-$3d$) x ray that is used for our overall normalization. It would make more sense if the radiationless transitions occurred instead of a (4-1) transition. Unfortunately, Lohs *et al*. [23] did not consider gold. Because the data of Hartmann *et al*. appear to be better than ours, we use their value of 75.6% for the yield of the ($4f$-$3d$) transition, instead of ours of 82.6%.

Now we turn to γ rays. First let us consider the prompt effects. Prompt neutron emission might produce γ rays, although mostly it is likely to lead to the ground state of ^{196}Au. Unfortunately, many levels in ^{196}Au are below 200 keV and cannot be observed. In addition, mixing in the muonic cascade between x rays and γ rays may result in transitions from ^{197}Au, although the energy might be shifted by the isomer effect. For ^{197}Au, the only one observed is the 279.01-keV level at an observed energy of 279.17(20) and intensity of 4.6(12)% per stop. Now this level could also be excited by the (n, n') reaction initiated by neutrons emitted from muon capture, but our experience in bismuth is that this background effect is small; we thus tentatively assign this γ ray to x ray mixing during the muonic cascade. This would not effect the cascade intensity as it just shifts transitions from one fine splitting level to another.

TABLE XIV. Observed γ-ray yields, per muon capture, for the reaction ^{127}I(μ^-, $\nu 4n\gamma$)^{123}Te, ^{127}I(μ^-, $\nu 5n\gamma$)^{122}Te, ^{127}I(μ^-, $\nu 6n\gamma$)^{121}Te.

Level in ^{123}Te (keV)	J^π	Transition branching ratio (%)	Transition energy (keV)	Observed γ-ray yield (%)
159.02	$3/2^+$	100	159.00	8(5)
489.81	$11/2^-$	100	330.78	1.0(5)
^{122}Te				
564.12	2^+	100	564.12	1.5(10)
1181.36	4^+	100	617.34	1.2(5)
^{121}Te				
212.19	$3/2^+$	100	212.19	1.0(5)

For the reaction ^{197}Au(μ^-, $\nu\gamma$)^{197}Pt, again there is the problem that there are a multitude of low energy levels, and we detect no obvious transitions. However, for the reaction ^{197}Au(μ^-, $\nu n\gamma$)^{196}Pt, there are many clear detections presented in Table XVIII, compared to the earlier results of Evans [4]; note that ^{196}Pt is bound up to 7.92 MeV, so even more transitions are possible. Now Evans used the normalization that the muonic ($4f$-$3d$) transition had a yield of 55% per stop (noting an uncertainty of 40%), whereas we have used 75.6%; thus we have renormalized Evans's results by $75.6/55 = 1.37$ to account for these different assumptions, and it improves the agreement significantly. The line at 326.35 keV in ^{196}Pt was not identified by Evans, even though it has a yield of 6.7(20)%. We illustrate the problem in Fig. 5. There is another strong line at 328.46 keV from ^{194}Pt with a yield of 13.9(28)%, also not reported by Evans. We had to fit the line shape to obtain these yields, fixing the known energies of each γ ray. Also in the figure are lines at 332.98 and 355.68 keV from ^{196}Pt, and a complex at 347 keV, which is mainly the ($2p$-$1s$) muonic x ray in aluminum.

The direct yields of the reaction ^{197}Au(μ^-, $\nu n\gamma$)^{196}Pt are given in Table XIX by taking into account the transition branching ratios and removing known cascading from the results in Table XVIII. We compare the direct yield with the spectroscopic factors from the reaction ^{197}Au(d,^{3}He)^{196}Pt

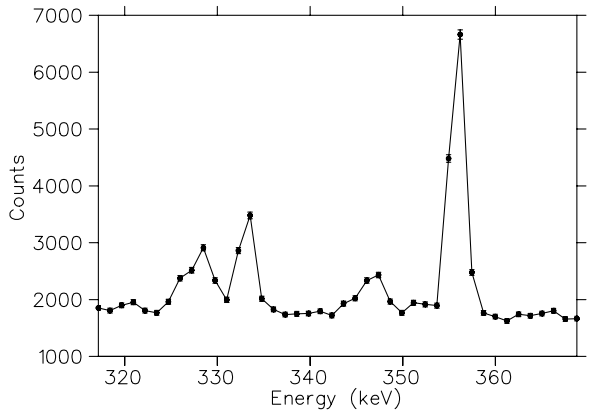

FIG. 5. Low-energy spectrum from muon capture in gold, illustrating the overlap between the γ ray at 326.35 keV from ^{196}Pt and that at 328.46 keV from ^{194}Pt. The yields were obtained by fixing the energies and then fitting standard line shapes.

TABLE XV. Estimates for the overall pattern of yields, all in percentages, for muon capture in ^{127}I.

Reaction	Observed γ-ray yield	Estimated ground-state transition	Missing yields	Total yield
^{127}I(μ^-, ν)^{127}Te	7(2)	–	1	8
^{127}I(μ^-, νn)^{126}Te	44(3)	10(10)	−2	52
^{127}I(μ^-, $\nu 2n$)^{125}Te	15(3)	2	1	18
^{127}I(μ^-, $\nu 3n$)^{124}Te	15(2)	1	−2	14
^{127}I(μ^-, $\nu 4n$)^{123}Te	8(5)	–	−3	5
^{127}I(μ^-, $\nu 5n$)^{122}Te	1.5(10)	1	–	2.5
^{127}I(μ^-, $\nu 6n$)^{121}Te	1.0(5)	–	−0.6	0.4
^{127}I(μ^-, $\nu 7n$)^{120}Te	–	–	0.1	0.1
^{127}I(μ^-, $\nu 8n$)^{119}Te	–	–	–	0.02
Total	91.5(7)	14(10)	−5.5	100

[10,42]. There is no obvious correlation between the two reactions. Unfortunately, there are no results for the reaction ^{197}Au(γ, p)^{196}Pt, and the high-energy electron studies of the reaction ^{197}Au(e, $e'p$)^{196}Pt from the Jefferson Lab [43] do not have sufficient energy resolution to be useful to us. It would be interesting to compare the yields to the 1373.60-keV level, but unfortunately it cascades to the 1270.21-keV level with a γ ray of only 103.3 keV, which is too low in energy for us to observe in this experiment.

For the reaction ^{197}Au(μ^-, $\nu 2n\gamma$)^{195}Pt, the nucleus ^{195}Pt has many low-lying levels; for the higher-lying levels, we have no convincing identification. For the reaction ^{197}Au(μ^-, $\nu 3n\gamma$)^{194}Pt, there are several clear γ rays, and these are presented in Table XX. Evans did not describe the 328-keV line, but most of the other levels cascade through this one, so our yield is reasonable; see Fig. 5.

TABLE XVI. The muonic Lyman (or K) and Balmer (or L) series for gold, giving the observed energy and the absolute intensity per muon stop, normalized to 95% for the sum of the K series. Comparison is made to the experimental results of Hartmann *et al.* [21]. The estimated energies in curly brackets are corrected point nucleus values.

	Energy (keV)	Intensity (%)	Previous results [21] (%)
	Lyman μ x rays		
$2p_{1/2}$-$1s_{1/2}$	5591.0[a]	34.2(30)	
$2p_{3/2}$-$1s_{1/2}$	5763.1[a]	55.2(40)	Sum is 89.9(37)
$3p_{1/2}$-$1s_{1/2}$	{8085}	1.6(16)	
$3p_{3/2}$-$1s_{1/2}$	{8128}	3.9(20)	Sum is 4.5(4)
	Balmer μ x rays		
$3d_{3/2}$-$2d_{3/2}$	2302(2)	4.1(17)	
$3d_{5/2}$-$2d_{3/2}$	2341.2(2)	45.8(35)	
$3d_{3/2}$-$2d_{1/2}$	2477.8[a]	30.3(36)	Sum is 80.4(27)
$4d_{5/2}$-$2d_{3/2}$	3202(5)	3.3(10)	
$4d_{3/2}$-$2d_{1/2}$	3356(5)	3.7(12)	Sum is 5.6(5)
$5d_{5/2}$-$2d_{3/2}$	{3601}	1.3(13)	–
$5d_{3/2}$-$2d_{1/2}$	{3762}	1.0(10)	–

[a]Center of gravity of the observed line, taken from Powers *et al.* [17] and used as an energy calibration.

For the reaction ^{197}Au(μ^-, $\nu 3n\gamma$)^{194}Pt, many transitions go to the 328-keV level, so that at least half (viz. 7.2%) is cascading; similarly the 811-keV level appears to be entirely cascading. For the reaction ^{197}Au(μ^-, $\nu 4n\gamma$)^{193}Pt, the nucleus ^{193}Pt has 16 levels below 500 keV and we have no identification of any of them. For the reaction ^{197}Au(μ^-, $\nu 5n\gamma$)^{192}Pt, there are bumps at transitions corresponding to the first and second excited state with yields of 1(1)%, but this is not very convincing. From systematics of other elements, one would expect a yield of ∼3% for this reaction, including the ground-state transition.

We have also searched for proton and α-producing reactions, but have observed no yield. This is consistent with the activation results of Wyttenbach *et al.* [39], which indicate that the total yield for gold (including the ground state) would be 0.02% for the (μ, νp) reaction, 0.1% for the (μ, νpn) reaction, 0.1% for the (μ, $\nu p2n$) reaction, and ∼0.01% for the (μ, $\nu p3n$) reaction.

We can now summarize our results in Table XXI for muon capture in gold, giving our results, estimates for the ground-state transitions, and estimates for the yield of the missing transitions, using the results of MacDonald *et al.* [40], as analyzed by Measday [2], as a guide for the total neutron yields, and the calculations of Lifschitz and Singer [41] for the higher multiplicity modes. We are clearly missing a lot of the yield, most probably because of the high level density in the odd platinum isotopes.

VI. RESULTS FOR BISMUTH

Bismuth was chosen as a target because it is one of the heaviest nuclides and has only one isotope. It also has a fairly small hyperfine effect. The x rays have been studied by Bardin *et al.* [19] and Powers [20] and are important for energy calibration; however, the intensities were not discussed in these publications, because their main interest was in nuclear charge

TABLE XVII. The muonic Paschen (or M) and Brackett (or N) series for gold, giving our observed energy, compared to previous values [16,17], and the absolute intensity per muon stop, with the 5% radiationless transitions added back in. Comparison for the intensity is made to the experimental results of Hartmann *et al*. [21]. The estimated energies in curly brackets are corrected point nucleus values.

	Energy (keV)	Previous energy [16,17]	Intensity (%)	Previous results [21] (%)
		Paschen μ x rays		
$4f_{5/2}$-$3d_{3/2}$	870.11(10)	870.02(9)	47.9(12)	
$4f_{7/2}$-$3d_{5/2}$	899.27(10)	899.16(9)	34.7(12)	Sum is 75.6(15)
$5f_{5/2}$-$3d_{3/2}$	1267(1)		4.4(13)	
$5f_{7/2}$-$3d_{5/2}$	1299(1)		1.8(8)	Sum is 8.0(3)
$6f_{5/2}$-$3d_{3/2}$	{1482}		0.4(4)	
$6f_{7/2}$-$3d_{5/2}$	{1516}		0.4(4)	Sum is 3.3(3)
$7f_{5/2}$-$3d_{3/2}$	{1612}		0.8(5)	
$7f_{7/2}$-$3d_{5/2}$	{1647}		0.4(4)	Sum is 1.3(3)
		Brackett μ x rays		
$5g_{9/2}$-$4f_{7/2}$	400.15(15)	400.14(5)	38.8(21)	
$5g_{7/2}$-$4f_{5/2}$	405.58(15)	405.65(5)	30.6(21)	Sum is 67.6(25)
$6g_{9/2}$-$4f_{7/2}$	615.5(4)		6.9(20)	
$6g_{7/2}$-$4f_{5/2}$	621.7(4)		5.8(20)	Sum is 9.2(4)
$7g_{9/2}$-$4f_{7/2}$	744.9(5)[a]		2.9(29)	
$7g_{7/2}$-$4f_{5/2}$	752.1(5)		2.3(11)	Sum is 2.6(1)
$8g_{9/2}$-$4f_{7/2}$	{829}		0.6(3)	
$8g_{7/2}$-$4f_{5/2}$	{836}		1.3(6)	Sum is 1.1(4)
$9g_{9/2}$-$4f_{7/2}$	{887}		0.4(4)	–
$9g_{7/2}$-$4f_{5/2}$	{895}		0.2(2)	–

[a]Same energy as a γ ray from I(n, n').

radii, and x ray coupling to nuclear levels. The measurements of Schröder *et al*. [44] were taken with a NaI(Tl) detector, so are not much help for us. The muon capture γ rays were observed by Backenstoss *et al*. [3] and we are in good agreement wth their results. For bismuth there is not only the possibility of prompt radiationless transitions giving neutrons but also nuclear excitation during the x-ray cascade. For this nucleus these transitions occur instead of the x ray, so must be taken into account. The γ-ray energies are also significantly shifted and have been the subject of three earlier studies, so we can compare our results with theirs.

Thus we model the cascade as follows. The muon reaches the $3d$ level with normal x ray and Auger cascading; then there is a 8.5% loss due to nuclear level excitation, removing some of the $(3d$-$2p)$ muonic transition, plus a 7% loss due to prompt neutron emission. At the $2p$ level the nuclear excitation effect is regained, thus the Lyman series has only the loss due to the prompt neutrons and is normalized to 93%. We note in passing that for both gold and bismuth the experimental $(3d$-$2p)$ yields are slightly high, and the $(2p$-$1s)$ yields are slightly low in absolute terms, using the $(4f$-$3d)$ x ray as a normalization and our efficiency calibration; see Fig. 2. This could be that our cascade model is wrong or that the efficiency relation, i.e., Eqs. (1) and (2), is not adequate above 3 MeV, and the efficiency falls off slightly faster. This is not of major concern but a warning for others who may need precision results.

The results for the Lyman and Balmer series in bismuth are given in Table XXII. We follow the cascade to more x rays than in gold, as the spectrum has 4 times more statistics. There are no other results to compare with, but the results are consistent with the overall pattern in gold.

In Table XXIII we present the muonic Paschen (or M) and Brackett (or N) series for bismuth. For these higher transitions, we have added back the 7% radiationless effect and the 8.5% nuclear level excitation. The overall pattern is consistent with the results for gold. Note that the normalization for ^{209}Bi is that the $(4f$-$3d)$ muonic x ray has a yield of 77(7)% per stop; Backenstoss *et al*. used 72%, which is consistent, so we do not renormalize their yields. We also give our observed energies for those cases with an adequate yield. The $(4f$-$3d)$ and $(5g$-$4f)$ energies were precisely measured by Backenstoss *et al*. [16,45,46] with the aim of determining the effect of vacuum polarization on the muonic levels. We see that our values are in excellent agreement, giving us confidence in our energy calibration procedures.

We now consider the effects of nuclear excitation during the muonic cascade. We estimate that the 2564-keV level is excited for 3.2% of the stops and the 2741-keV level is excited for 5.3% of the stops. The 2564-keV level de-excites 100% of the time by a γ ray that is shifted up in energy by 3 keV in the muonic atom. The 2741-keV level has a more complicated de-excitation; 55% of the time it de-excites to the ground state with a γ that is shifted up in energy by 6 keV, 38% of the time there is a cascade through the 1608.5-keV level with the two γ of 1132 and 1608 keV shifted up by 3 keV, and 7% of the time there is a cascade of 140.1, 992.35, and 1608.5 keV (energies of the unperturbed nuclear levels). Thus this cascade occurs for only about 0.3% of μ stops; the 140-keV line is too low in energy and the 992-keV line

TABLE XVIII. Observed γ-ray yields, per muon capture, for the reaction ^{197}Au(μ^-, $\nu n\gamma$)^{196}Pt , compared to the previous results from Evans [4], renormalized by a factor of 1.37.

Level in ^{196}Pt (keV)	J^π	Transition branching ratio (%)	Transition energy (keV)	Observed γ-ray yield (%)	Previous results Ref. [4] (%)
355.68	2^+	100	355.68	47.1(30)	49(7)
688.69	2^+	100	332.98	15.8(20)	15.1(2.7)
876.87	4^+	100	521.18	16.6(16)	14.5(16)
1015.04	3^+	95	326.35	6.7(20)	
1135.31	0^+	72	779.63	1.3(3)	
		28	446.61	0.5(5)	
1270.21	5^-	100	393.35	7.4(10)	6.6(14)
1293.31	4^+	13	937.62	<0.9	
		75	604.62	4.4(1.9)	
		13	416.44	<2[a]	
1361.59	2^+	35	1005.89	1.9(6)	
		44	672.90	0.6(10)	
1373.60	7^-	100	103.3	?[b]	
1402.73	0^+	100	1047.04	1.4(7)	
1447.04	3^-	64	1091.33	3.7(13)	2.5(11)
		13	758.36	2.1(10)[c]	
1604.49	2^+	47	1248.84	<1.1	
		19	915.80	0.8(4)[d]	
		21	727.58	1.0(5)[d]	
1820.69	9^-	100	447.1	1.3(7)	
1847.35	2^+	94	1491.60	0.7(4)	

[a]Mixed with I(n, n') at 417.95 keV, and Ni($4d$-$2p$) at 415.6 and 420.4 keV.
[b]E_γ too low to be observed.
[c]Appears to be contaminated.
[d]Doubtful identification.

TABLE XIX. Our results for the direct excitation of a level in the reaction ^{197}Au(μ^-, $\nu n\gamma$)^{196}Pt, taking into account the known cascading, compared to the spectroscopic factors from the reaction ^{197}Au(d,^{3}He)^{196}Pt.

Level in ^{196}Pt (keV)	Known cascading (%)	Direct yield per capture (%)	C^2S from the reaction ^{197}Au(d,^{3}He)^{196}Pt
0			0.24
355.68	42.4(31)	4.7(43)	0.21
688.69	14.2(29)	1.6(35)	0.14
876.87	8.6(11)	8.0(23)	$\leqslant$0.04
1015.04	0.6(3)	6.5(32)	$\leqslant$0.04
1135.31	–	1.8(4)	$\leqslant$0.02
1270.21	1.6(7)[a]	5.8(12)[a]	–
1293.31	–	5.9(25)	0.20
1361.59	–	3.2(20)	–
1373.60	–	?	0.65
1402.73	–	1.4(7)	0.07
1447.04	–	5.8(20)	–
1604.49	–	2(1)	0.13
1820.69	–	1.3(7)	–
1847.35	–	0.7(4)	–

[a]There could also be a major contribution of cascading from the level at 1373.60 keV.

TABLE XX. Observed γ ray yields, per muon capture, for the reaction ^{197}Au(μ^-, $\nu 3n\gamma$)^{194}Pt, compared to the previous result from Evans [4], renormalized by a factor of 1.37.

Level in ^{194}Pt (keV)	J^π	Transition branching ratio (%)	Transition energy (keV)	Observed γ-ray yield (%)	Previous result Ref. [4] (%)
328.45	2^+	100	328.46	13.9(28)	
622.00		88	293.56	1.6(8)	
811.32		100	482.83	5.6(9)	4.4(11)
1373.94		99	562.64	3.0(10)	
1411.86		100	600.54	3.9(14)	

is drowned by the 997 keV Bi ($4f_{5/2}$-$3d_{3/2}$) muonic x ray. Our results are presented in Table XXIV and compared to previous results [24–26]. We also illustrate this in Fig. 6, which shows the 2571- and 2746-keV lines; also seen are the bismuth ($3d_{5/2}$-$2p_{3/2}$) doublet at 2555 keV, the ($3d_{3/2}$-$2p_{1/2}$) x ray at 2701 keV, and the huge capture γ ray from ^{208}Pb at 2614.5 keV. (Note that for illustrative purposes, this spectrum was taken from the histogram with a gain of 5 keV per channel, but our data analysis used the spectrum with 1.3 keV per channel, and thus with better definition for the isomer shift lines at 2771 and 2746 keV.) In Table XXIV we see that the energy results, the focus of all previous experiments, are in good agreement. Our result for the 2741-keV line came at a break in our spectra, so our result is not very accurate, and so most of the time we used the previous results as a calibration. For us the intensities are more important; there is reasonable agreement except that our value for the 1611-keV line is somewhat high; the line is also broadened symmetrically. In Table 1 of Walter [47], there is the implication that the 1608-keV level could be excited independently by 1.3(7)%, using the data of Backe *et al.* [25]. This is not discussed, nor is there any obvious coupling, but it is a possibility. There might be a contamination from a neutron capture in

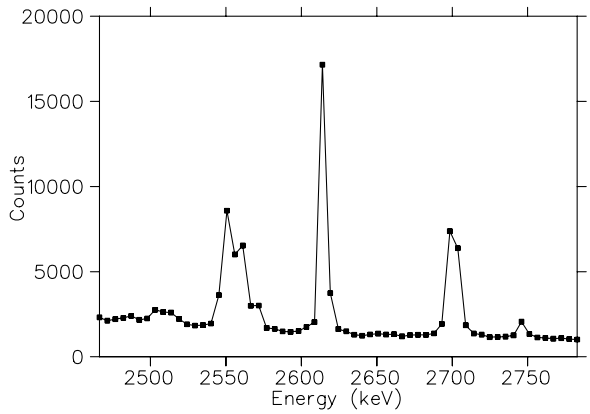

FIG. 6. A spectrum from bismuth, illustrating the strength of the 2614.5-keV γ ray from ^{208}Pb. The peaks at 2555 and 2701 are bismuth muonic x rays, the ($3d_{5/2}$-$2p_{3/2}$) and ($3d_{3/2}$-$2p_{1/2}$), respectively. Peaks at 2571 and 2746 are the isomer shifted γ rays from ^{209}Bi (see text and Table XXIV). (Note that this spectrum is binned for illustrative purposes.)

TABLE XXI. Estimates for the overall pattern for yields, all in percentages, for muon capture in ^{197}Au.

Reaction	Observed γ-ray yield	Estimated ground-state transition	Missing yields	Total yield
^{197}Au(μ^-, ν)^{197}Pt	–	–	8	8
^{197}Au(μ^-, νn)^{196}Pt	48(4)	2	−2	48
^{197}Au(μ^-, $\nu 2n$)^{195}Pt	–	2	18	20
^{197}Au(μ^-, $\nu 3n$)^{194}Pt	14(3)	1	−1	14
^{197}Au(μ^-, $\nu 4n$)^{193}Pt	–	2	4	6
^{197}Au(μ^-, $\nu 5n$)^{192}Pt	–	1	2	3
^{197}Au(μ^-, $\nu 6n$)^{191}Pt	–	0.8	–	0.8
^{197}Au(μ^-, $\nu 7n$)^{190}Pt	–	0.2	–	0.2
^{197}Au(μ^-, $\nu 8n$)^{189}Pt	–	–	–	0.05
Total	62(5)	9	29	100

iron at 1612.78 keV, but this does not seem sufficient to explain the discrepancy. Thus we have neither a fully satisfactory explanation nor identification. It is a small effect for our purposes, so we disregard this measurement and deduce the intensities given above, viz. 3.2(3)% excitation of the 2564 level and 5.3(6)% excitation of the 2741-keV level.

For the other prompt effect, viz. neutron emission, we found two γ rays in ^{208}Bi, the 601.6-keV ground-state transition, with a yield of 0.8(5)%, and the 565.3-keV transition from the 628.6-keV level, with a 0.7(3)% yield. These are consistent with the prompt neutron results. There are several other possible γ rays, but all would have a low yield and are hidden by nearby more intense lines.

TABLE XXII. The muonic Lyman (or K) and Balmer (or L) series for bismuth, giving the observed energy, compared to previous results [16], and the absolute intensity per muon stop, normalized to 93% for the sum of the K series, and 76.2% for the L series. The estimated energies in curly brackets are corrected point nucleus values.

	Energy (keV)	Previous energy [16] (keV)	Intensity (%)
	Lyman μ x rays		
$2p_{1/2}$-$1s_{1/2}$	5841.5(30)[a]		36.1(15)
$2p_{3/2}$-$1s_{1/2}$	6032.4(30)[a]		48.6(15)
$3p_{1/2}$-$1s_{1/2}$	8539(10)		2.3(3)
$3p_{3/2}$-$1s_{1/2}$	8584(10)		2.6(3)
$3p_{3/2}$-$1s_{1/2}$	8628(10)		0.7(4)
$4p$-$1s$	{9468/9521}		1.0(7)
$5p$-$1s$	{9945/9973}		0.3(6)
$6p$-$1s$	{10201/10218}		1.2(12)
	Balmer μ x rays		
$3d_{3/2}$-$2p_{3/2}$	2504(2)	2501.8(6)	1.5(8)
$3d_{3/2}$-$2p_{3/2}$	2549.6(3)	2549.88(15)	22.5(11)
$3d_{5/2}$-$2p_{3/2}$	2558.9(3)		18.4(11)
$3d_{3/2}$-$2p_{1/2}$	2700.3(2)	2700.5(2)	26.7(11)
$4d_{5/2}$-$2p_{3/2}$	3510(1)		4.0(14)
$4d_{3/2}$-$2p_{1/2}$	3679(1)		2.2(6)
$5d_{5/2}$-$2p_{3/2}$	{3951}		0.3(6)
$5d_{3/2}$-$2p_{1/2}$	{4132}		0.5(5)
$6d_{5/2}$-$2p_{3/2}$	{4191}		<0.7
$6d_{3/2}$-$2p_{1/2}$	{4376}		<0.7

[a]Center of experimental line, taken from Bardin *et al.* [19] and used as a calibration.

TABLE XXIII. The muonic Paschen (or M) and Brackett (or N) series for bismuth, giving the observed energy, compared to previous results [16,45,46], and the absolute intensity per muon stop, with the 7% radiationless transitions added back in, as well as the 8.5% nuclear excitation loss in the ($3d$-$2p$) transition. The estimated energies in curly brackets are corrected point nucleus values.

	Energy (keV)	Previous energy [16] (keV)	Intensity (%)
	Paschen μ x rays		
$4f_{7/2}$-$3d_{5/2}$	961.3(2)	961.18(25)	42.7(29)
$4f_{5/2}$-$3d_{3/2}$	996.8(2)	996.67(25)	34.5(24)
$5f_{7/2}$-$3d_{5/2}$	1400.4(5)		3.9(6)
$5f_{5/2}$-$3d_{3/2}$	1440.2(5)		2.9(8)
$6f_{7/2}$-$3d_{5/2}$	1640.1(5)		2.2(6)
$6f_{5/2}$-$3d_{3/2}$	{1681.0}[a]		1.2(10)
$7f_{7/2}$-$3d_{5/2}$	1783(2)		0.4(2)
$7f_{5/2}$-$3d_{3/2}$	1826(2)		0.8(6)
$8f_{7/2}$-$3d_{5/2}$	1876(2)		1.0(6)
$8f_{5/2}$-$3d_{3/2}$	1920(2)		0.7(7)
	Brackett μ x rays		
$5g_{7/2}$-$4f_{5/2}$	442.0(1)	442.11(5)	39.8(19)
$5g_{9/2}$-$4f_{7/2}$	448.7(1)	448.83(5)	32.0(19)
$6g_{7/2}$-$4f_{5/2}$	679.7(1)		4.8(10)
$6g_{9/2}$-$4f_{7/2}$	687.6(2)		3.7(10)
$7g_{7/2}$-$4f_{5/2}$	823.4(5)		1.4(5)
$7g_{9/2}$-$4f_{7/2}$	832.0(5)		1.2(6)
$8g_{7/2}$-$4f_{5/2}$	{916.3}		0.7(6)
$8g_{9/2}$-$4f_{7/2}$	{924.4}		0.5(3)
$9g_{7/2}$-$4f_{5/2}$	{980.2}		<0.5
$9g_{9/2}$-$4f_{7/2}$	{988.5}		<0.4
$10g_{7/2}$-$4f_{5/2}$	{1025.9}		0.4(4)
$10g_{9/2}$-$4f_{7/2}$	{1034.3}		0.2(2)

[a]At the same energy as, and dominated by, the double escape peak of the Bi x ray ($3d_{3/2}$-$2p_{1/2}$).

TABLE XXIV. Comparison of results for the isomer shift and intensity, per μ stop, in bismuth [24–26].

Nuclear energy (keV)	Lee *et al.* [24]	Backe *et al.* [25]	Rüetschi *et al.* [26]	Our results	Previous intensities [24,25] (%)	Our intensities (%)
140.13(1)					(0.3)	
1132.46(5)	1135.51(13)	1135.04(18)	1135.05(13)	1135.3(2)	1.7(3)	1.9(4)
1608.53(6)	1610.97(13)	1611.21(+12−45)	1612.30(27)	1611.3(2)	3.0(6)	5.7(5)
2564.14(9)	2570.47(25)	2570.47(25)	2570.86(24)	2570.6(2)	2.7(8), 3.1	3.5(8)
2741.03(6)	2746.41(22)	2747.23(24)	2747.23(22)	2746.2(5)	2.5(4)	3.1(5)

We have marginal observations of γ rays from the ^{209}Bi(μ^-, $\nu\gamma$)^{209}Pb reaction; the 778.8-keV line at a yield of 0.8(2)%, the 1423-keV transition with 0.8(8)% yield, and finally the 2464-keV line at 0.9(5)%; we have limits of <0.5% on seven other potential low-lying levels. The main excitation is probably going to high excitation levels.

TABLE XXV. Our results for the reaction ^{209}Bi(μ^-, $\nu n\gamma$)^{208}Pb, with absolute yields per muon capture, compared to the earlier results of Backenstoss *et al.* [3].

Level in ^{208}Pb (keV)	J^π	Transition branching ratio (%)	Transition energy (keV)	Observed γ-ray yield (%)	Previous results Ref. [3] (%)
2614.55	3^-	100	2614.53	45(4)	43(7)
3197.74	5^-	100	583.19	24(2)	22.2(15)
3475.11	4^-	34	277.35	1.2(6)	2.7(8)
		66	860.56	2.5(6)	
3708.44	5^-	98	510.77	?[a]	
3919.80	$(6)^-$	44	211.40	2.7(8)	
		56	722.04	0.6(3)	
3946.44	$(4)^-$	100	748.7	2.0(7)	
3960.96	5^-	28	252.61	1.2(8)	
		70	763.13	1.0(4)	
3995.7	$(5)^-$	22	798.0	0.2(2)	
		78	1381.1	1.1(5)	
4050.5	$(3)^-$	100	1436.0	<1.1	
4085.4	2^+	100	4085.4	0.7(5)	
4125.31	$(4, 5)^-$	21	650.1	0.6(4)	
		79	927.6	1.0(4)	
4180 41	5^-	10	705.2	<0.3	
		90	982.7	0.7(4)	
4205.4	$(6)^-$	100	1008	0.9(5)	
4262.4		22	553	0.5(5)	
		29	786.8	0.6(4)	
		49	1647.9	1.3(4)	
4296.17		50	587.7	0.8(5)	
		50	821.2	<0.3	
4323.2		100	1125.8	1.5(3)	
4358.46		71	883.3	0.3(3)	
		25	1160.8	0.5(5)	
4382.9		100	1185.1	1.4(4)	
4422		100	1225	1.4(6)	
4480.5		100	1282.8	0.7(3)	
4854.7		100	770	0.3(2)	

[a]Totally lost in the 511-keV annihilation radiation.

As usual for the reaction ^{209}Bi(μ^-, $\nu n\gamma$)^{208}Pb, we have very clear detections and many more than the earlier work of Backenstoss *et al.* [3]; see Table XXV.

In Table XXVI we give the direct excitation of the levels in ^{208}Pb from the reaction ^{209}Bi(μ^-, $\nu n\gamma$)^{208}Pb by accounting for the transition branching ratios and the known cascading; we can then compare to reactions such as ^{209}Bi(d,^{3}He)^{208}Pb, ^{209}Bi(e, $e'p$)^{208}Pb, and ^{209}Bi(γ, p)^{208}Pb. In lighter elements the (γ, p) reaction has been found to correlate quite well with the (μ^-, νn) reaction. However, for bismuth, the data of Uegaki *et al.* [5] on ^{209}Bi(e, $e'p$)^{208}Pb and ^{209}Bi(γ, p)^{208}Pb are not sufficiently general to be useful, and even if modern techniques

TABLE XXVI. Results for the direct excitation of the levels in ^{208}Pb from the reaction ^{209}Bi(μ^-, $\nu n\gamma$)^{208}Pb, obtained by subtracting known cascading from the results in Table XXV. We compare with the results of the reaction ^{209}Bi(d,^{3}He)^{208}Pb.

Level in ^{208}Pb (keV)	Known cascading (%)	Direct yield per capture (%)	C^2S from the reaction ^{209}Bi(d,^{3}He)^{208}Pb
0	46(4)	3[a]	0.075
2614.55	28.7(21)	16.3(45)	0.18
3197.74	16.8(20)	7.2(30)	0.08
3475.11	2.3(7)	1.4(11)	v. small
3708.44	2.5(6)	?[b]	0.36+0.08
3919.80	–	1.8(8)	v. small
3946.44	–	2.0(7)	0.67+0.12
3960.96	–	2.1(7)	0.43+0.08
3995.7	–	1.3(5)	0.04
4050.5	–	<1.1	v. small
4085.4	0.3(2)	0.4(5)	v. small
4125.31	–	1.7(6)	0.04+0.51
4180 41	–	0.8(5)	<0.07
4205.4	–	0.9(5)	0.07
4262.4	–	2.5(6)	0.11+0.75
4296.17	–	1.0(5)	0.10+0.25
4323.2	–	1.5(3)	0.10
4358.46	–	0.8(8)	0.02+0.22
4382.9	–	1.4(4)	1.00
4422	–	1.4(6)	0.40
4480.5	–	0.7(3)	0.14
4854.7	–	0.3(2)	0.09

[a]Estimate, using the (d,^{3}He) reaction as a guide.
[b]Totally lost in the 511-keV annihilation radiation.

TABLE XXVII. Our γ-ray yields for the reaction ^{209}Bi(μ^-, $\nu 2n\gamma$)^{207}Pb, per muon capture, compared to the earlier results of Backenstoss *et al*. [3].

Level in ^{207}Pb (keV)	J^π	Transition branching ratio (%)	Transition energy (keV)	Observed γ-ray yield (%)	Previous results Ref. [3] (%)
569.70	$5/2^-$	100	569.70	22.4(19)	13.3(20)
897.80	$3/2^-$	99	897.78	7.2(11)	6.0(30)
1633.37	$13/2^+$	100	1063.66	9.5(9)[a]	
2339.95	$7/2^-$	98	1770.24	2.4(6)	
2623.5	$5/2^+$	100	1725.7	1.3(6)	
2662.4	$7/2^+$	100	2092.7	1.7(6)	
2727(1)[b]	$9/2^+$	86	1095	2.8(4)	
		14	389	2.0(8)	

[a]This level has a lifetime of 0.81 s, so this is a lower limit on the yield. It also cascades through the 570-keV level.
[b]Our observations give the energy as 2728.0(5) keV.

were used, the Coulomb effects would probably make the comparison meaningless.

However, there are recent useful results for the reaction ^{209}Bi($e, e'p$)^{208}Pb from NIKHEF and some results on the reaction ^{209}Bi(γ, p)^{208}Pb at $E_\gamma = 48$ MeV from MAX-lab [48]. This γ-ray energy is sufficiently high to avoid major worries from the Coulomb interaction. In both reactions they observe strong excitation of levels in ^{208}Pb at 4.1 and 5.4 MeV. Below 4 MeV there is very little feeding. Now this is consistent with the results on the reaction ^{209}Bi(d,^{3}He)^{208}Pb that have a better resolution and would suggest three peaks at 4.0, 5.2, and 5.6 MeV, but the second two would coalesce with the resolution obtained in the ^{209}Bi(γ, p)^{208}Pb and ^{209}Bi($e, e'p$)^{208}Pb reactions. Thus we can take the (d,^{3}He) results and ask if we observe any of these levels, remembering that ^{208}Pb is bound up to 7.37 MeV, so all these levels decay by γ-ray emission. For the 4.0 MeV region, we see some correlation. For the 5.2 and 5.6 MeV regions the γ-ray cascades are poorly known for levels at 4894, 5074, 5163, 5195, 5212, 5320, 5342, 5494, 5547, 5679, and 5722 keV; the only one for which there is information is the level at 5547 keV that has a 100% cascade through the first excited state at 2614.55 keV, producing a 2932.5 keV γ ray. We actually have a marginal identification with a yield of 0.6(3)%. Now let us make a rash assumption that all these levels cascade through the first excited state, then we have another marginal observation, also of 0.6(3)% for the 5679-keV level with a γ ray at 3064.5 keV. Under this assumption, we do not observe the levels at 4894, 5074, 5212, 5342, 5494, and 5722 keV. The levels at 5163, 5195, and 5320 would produce

TABLE XXVIII. Results for the direct excitation of the levels in ^{207}Pb from the reaction ^{209}Bi(μ^-, $\nu 2n\gamma$)^{207}Pb, obtained by subtracting known cascading from the results in Table XXVII.

Level in ^{207}Pb (keV)	Known cascading (%)	Direct yield per capture (%)
569.70	13.6(12)	8.8(23)
897.80	1.3(6)	5.9(13)
1633.37	3.7(5)	5.8(10)
2339.95	0.6(1)	1.8(6)
2623.5	–	1.3(6)
2662.4	–	1.7(6)
2727(1)	–	3.5(5)

TABLE XXIX. Our γ-ray yields for the reaction ^{209}Bi(μ^-, $\nu 3n\gamma$)^{206}Pb, per muon capture, compared to the earlier results of Backenstoss *et al*. [3].

Level in ^{206}Pb (keV)	J^π	Transition branching ratio (%)	Transition energy (keV)	Observed γ-ray yield (%)	Previous results Ref. [3] (%)
803.05	2^+	100	803.06	9.3(10)	7.7(13)
1340.47	3^+	100	537.47	4.3(7)	3.0(8)
1466.80	2^+	77	663.75	0.8(3)	
		23	1466.78	0.5(5)	
1683.96	4^+	26	343.52	1.3(5)	
		74	880.98	3.6(8)	
1704.46	1^+	100	1704.45	0.4(2)	
1784.08	2^+	72	980.99	<0.5	
1997.65	4^+	74	657.18	1.0(4)	
2147.9	2^+	71	1345.88	0.5(3)	
2196.7		54	856.6	<0.4	
		42	1393.8	0.25(16)	
2200.14		100	516.18[a]	2.8(19)[a]	
2384.12		100	183.98	?[b]	
2647.77		94	1844.47	0.9(3)	
2658.4		100	458.1	0.40(15)	
2782.15		43	398.00	0.7(3)	
		53	1098.26	<2[c]	

[a]The γ-ray energy is close to the 511-keV annihilation line, so the uncertainty in the yield is large.
[b]E_γ too low to be observed.
[c]Drowned by a nickel background.

TABLE XXX. Results for the direct excitation of the levels in ^{207}Pb from the reaction ^{209}Bi(μ^-, $\nu 3n\gamma$)^{206}Pb, obtained by subtracting known cascading from the results in Table XXIX.

Level in ^{206}Pb (keV)	Known cascading (%)	Direct yield per capture (%)
803.05	10.6(11)	−1.3(15)
1340.47	2.8(5)	1.5(9)
1466.80	0.1	1.1(5)
1683.96	4.0(19)	0.9(22)
1704.46	–	0.4(2)
1997.65	–	1.4(5)
2147.9	–	0.7(4)
2196.7	–	0.6(4)
2200.14	1.1(3)	1.7(20)
2384.12	0.7(3)	?[a]
2647.77	–	1.0(4)
2658.4	–	0.40(15)
2782.15	–	1.6(7)

[a]E_γ too low to be observed.

TABLE XXXI. Our results for the reaction ^{209}Bi(μ^-, $\nu 4n\gamma$)^{205}Pb, with absolute yields per muon capture.

Level in ^{205}Pb (keV)	J^π	Transition branching ratio (%)	Transition energy (keV)	Observed γ-ray yield (%)
262.83	$3/2^-$	75	260.50	1.2(4)
		25	262.80	<0.4
576.19	$3/2^-$	74	573.85	<0.4
703.43	$7/2^-$	100	703.44	0.4(4)
761.43	$5/2^-$	54	759.1	0.4(3)
803.38	$(1/2, 3/2)^-$	65	540.6	0.8(4)
987.63	$9/2^-$	91	987.6	1.6(4)
1043.74		88	1043.75	0.8(3)[a]

[a]The energy of this line is slightly off, so it may have another identification.

a γ ray at the same energy as the bismuth ($3d$-$2p$) x ray, and so could not be observed. Note that if these levels are fed, and cascade through either the 2614.55- or 3197.74-keV levels, we would already have included their effects in our summations. If they had a direct transition to the ground state, the detector efficiency would be only 60% of that around 2.9 MeV, and so it would be difficult to distinguish a peak from the noise; we observe no clear peak at a sensitivity of about 0.5% yield. We must leave these speculations until more information is available but conclude that our results are consistent with a few % excitations in the 5 MeV region from muon capture.

In Table XXVII we present our results for the reaction ^{209}Bi(μ^-, $\nu 2n\gamma$)^{207}Pb, again there are many excellent identifications. Above the 2727-keV level some levels may have been observed with a yield of 0.3%, but all are <1%. Note that the level at 1633 keV has a lifetime of 0.81 s, thus the reason that we observe it is because we had a fairly high stop rate. As it cascades through the 570-keV level, the yield of this level is raised, too, which probably explains the difference between our results and those of Backenstoss *et al.*

Results for the direct excitation of the levels in ^{207}Pb from the reaction ^{209}Bi(μ^-, $\nu 2n\gamma$)^{207}Pb are given in Table XXVIII and are obtained by taking into account the transition branching ratios and subtracting the known cascading from the results in Table XXVII.

In Table XXIX we present our results for the reaction ^{209}Bi(μ^-, $\nu 3n\gamma$)^{206}Pb; again, there are many excellent identifications.

We present in Table XXX results for the direct excitation of the levels in ^{206}Pb from the reaction ^{209}Bi(μ^-, $\nu 3n\gamma$)^{206}Pb, obtained by subtracting known cascading from the results in Table XXIX.

In Table XXXI we present our results for the reaction ^{209}Bi(μ^-, $\nu 4n\gamma$)^{205}Pb; we have a few marginal identifications, even for the production of four neutrons. Cascading affects only the 263-keV level seriously; of its apparent yield of 1.6(5)%, 0.9(4)% is cascading, thus leaving 0.7(6)% direct feeding. The 576-keV level receives ~0.25% cascading from the 803-keV level, but we do not observe either the 227-keV feeding, nor the subsequent 574-keV de-exciting transition.

For the reaction ^{209}Bi(μ^-, $\nu 5n\gamma$)^{204}Pb, we have one identification, a yield of 1.2(4)% for the 374.72(7) transition from the 1274.00-keV level. This requires at least the same yield of the 899.17-keV transition, but this is hidden by a line from ^{207}Pb at 897.78 keV with a strong yield of ~6%. For the reaction ^{209}Bi(μ^-, $\nu 6n\gamma$)^{203}Pb, we have no identification, with limits around 0.5%. This is consistent with the activation results of Wyttenbach *et al.*, who obtained a yield of 1.50(15)% for this reaction, including the ground state, which is likely to dominate. They also obtained 0.14(2)% for the reaction ^{209}Bi(μ^-, $\nu 7n$)^{202}Pb, and 0.28(2)% for the reaction ^{209}Bi(μ^-, $\nu 8n$)^{201}Pb; both these yields are below our sensitivity. We have also searched for proton and α production reactions, which give thallium and mercury isotopes, but observe nothing, with limits of about 0.5%. Again this is what is expected.

We can now summarize our results in Table XXXII for muon capture in bismuth, giving our results, estimates for the ground-state transitions, and estimates for the yield of the missing transitions, using the results of MacDonald *et al.* [40], as analyzed by Measday [2], as a guide for the neutron yields, averaging the results for gold and lead, and the calculations of Lifschitz and Singer [41] for the higher multiplicity modes. Our own results are often more of a constraint than these other measurements, because we observe a total yield of 95(6)%,

TABLE XXXII. Estimates for the overall pattern of yields, in percentages, for muon capture in bismuth.

Reaction	Observed γ-ray yield	Estimated ground-state transition	Missing yields	Total yield
^{209}Bi(μ^-, ν)^{209}Pb	3(1)	–	2	5
^{209}Bi(μ^-, νn)^{208}Pb	46(4)	3	−2	47
^{209}Bi(μ^-, $\nu 2n$)^{207}Pb	30(3)	2	−3	29
^{209}Bi(μ^-, $\nu 3n$)^{206}Pb	10(3)	1	−2	9
^{209}Bi(μ^-, $\nu 4n$)^{205}Pb	5(1)	1	−1	5
^{209}Bi(μ^-, $\nu 5n$)^{204}Pb	1(1)	2	–	3
^{209}Bi(μ^-, $\nu 6n$)^{203}Pb	–	1.5	–	1.5
^{209}Bi(μ^-, $\nu 7n$)^{202}Pb	–	0.2	–	0.2
^{209}Bi(μ^-, $\nu 8n$)^{201}Pb	–	0.3	–	0.3
Total	95(6)	11	−6	100

which is one of the highest ever recorded, thus few transitions have been missed.

VII. SUMMARY AND CONCLUSIONS

Our results on muon capture have greatly expanded the information on the muonic cascades and for muon capture in iodine, gold, and bismuth. For the muonic x rays, we confirm the energies measured in previous experiments, which gives us confidence in our energy calibrations and thus the identification of γ rays from muon capture. For the x-ray intensities, our results are in fair agreement with the excellent study of Hartmann *et al*. [21] for gold. We obtained new information for iodine and bismuth and use these for our normalization of muon capture yields and for estimating the self absorption in the target.

For muon capture, we have observed many more γ-ray transitions than have been identified before and confirmed the importance of the emission of multiple neutrons for muon capture in heavy elements. In iodine and bismuth, we have direct observations of over 90% of the yield; the only previous measurements to achieve this completeness were those of Budick *et al*. [49–51], who identified 93.3(88)% of the yield for muon capture in ^{207}Pb. Their pattern of neutron multiplicity is very similar to ours for bismuth. For gold the $(\mu^-, \nu 2n)$ and $(\mu^-, \nu 4n)$ reactions were not observed, most likely because of the high level density in the product nuclei.

Although we have identified many new γ rays, there are always a few that we cannot attribute to a reaction; some, of course, may be background or even noise. In iodine we detected unknown lines at 237.1, 339.5, 431.3, 703.3, 744.4, 917.5, 1574.2, and 1722.9 keV; in gold there were lines at 583.4, 933.7, and 1044.5 keV; in bismuth at 226.5, 229.8, 279.7, 525.5, 531.6, 789.8, 911.6, 941.4, 951.5, 1485, and 1508 keV. All have yields of between 0.5 and 1%.

To progress further with muon capture in heavy elements will be difficult. Not only would the experimental spectra need much higher statistics, but studies of background lines would need to match any increased sensitivity. Perhaps more important, however, is that we were already limited by present knowledge concerning energy levels and transition branching ratios. Thus there is still a need for expansion of the general data base of nuclear properties.

ACKNOWLEDGMENTS

We thank the many people who contributed to the successful completion of this experiment: E. Gete, T. P. Gorringe, J. Lange, B. A. Moftah, and M. A. Saliba, who helped set up the original experiment on nitrogen and took some shifts, too. J. Chuma wrote the program PHYSICA, which was used for the data analysis, and also wrote some of the macros specifically for this analysis. Of course, in a major laboratory like TRIUMF, many people help by keeping the cyclotron operating and preparing the experimental area for each experiment; the financial contribution for this essential activity is provided by the National Research Council of Canada. Finally, we thank the Natural Sciences and Engineering Research Council, Canada, for providing grants OGP0090780 and 240164-01, which made the experiment possible.

[1] D. F. Measday and T. J. Stocki, Phys. Rev. C **73**, 045501 (2006).
[2] D. F. Measday, Phys. Rep. **354**, 243 (2001).
[3] G. Backenstoss, S. Charalambus, H. Daniel, W. D. Hamilton, U. Lynen, Ch. von der Malsburg, G. Poelz, and H. P. Povel, Nucl. Phys. **A162**, 541 (1971).
[4] H. J. Evans, Nucl. Phys. **A207**, 379 (1973).
[5] J. Uegaki, K. Shoda, M. Sugawara, and T. Saito, Nucl. Phys. **A371**, 93 (1981).
[6] B. H. Wildenthal and E. Newman, Nucl. Phys. **A118**, 347 (1968).
[7] J. Ott, C. Doll, T. von Egidy, R. Georgii, M. Grinberg, W. Schauer, R. Schwengner, and H.-F. Wirth, Nucl. Phys. **A625**, 598 (1997).
[8] M. Vergnes, G. Berrier-Ronsin, G. Rotbard, J. Vernotte, H. Langevin-Joliot, E. Gerlic, J. van de Wiele, J. Guillot, and S. Y. van der Werf, Phys. Lett. **B107**, 349 (1981).
[9] N. Blasi, M. N. Harakeh, W. A. Sterrenburg, and S. Y. van der Werf, Phys. Rev. C **31**, 653 (1985).
[10] H. Langevin-Joliot, E. Gerlic, J. Guillot, J. van de Wiele, S. Y. van der Werf, and N. Blasi, Nucl. Phys. **A462**, 221 (1987).
[11] E. A. McLatchie, C. Glashausser, and D. L. Hendrie, Phys. Rev. C **1**, 1828 (1970).
[12] G. Mairle *et al*., Phys. Lett. **B121**, 307 (1983).
[13] R. M. Klein, Ph.D. thesis, Universität Mainz, 1988.
[14] G. Fricke, C. Bernhardt, K. Heilig, L. A. Schaller, L. Schellenberg, E. B. Shera, and C. W. de Jager, At. Data Nucl. Data Tables **60**, 177 (1995).
[15] W. Y. Lee, S. Bernow, M. Y. Chen, S. C. Cheng, D. Hitlin, J. W. Kast, E. R. Macagno, A. M. Rushton, and C. S. Wu, Nucl. Phys. **A167**, 652 (1971).
[16] R. Engfer, H. Schneuwly, J. L. Vuilleumier, H. K. Walter, and A. Zehnder, At. Data Nucl. Data Tables **14**, 509 (1974).
[17] R. J. Powers, P. Martin, G. H. Miller, R. E. Welsh, and D. A. Jenkins, Nucl. Phys. **A230**, 413 (1974).
[18] C. Bernhardt, Ph.D. thesis, Universität Mainz, 1990.
[19] T. T. Bardin, R. C. Cohen, S. Devons, D. Hitlin, E. Macagno, J. Rainwater, K. Runge, C. S. Wu, and R. C. Barrett, Phys. Rev. **160**, 1043 (1967).
[20] R. J. Powers, Phys. Rev. **169**, 1 (1968).
[21] F. J. Hartmann, R. Bergmann, H. Daniel, H.-J. Pfeiffer, T. von Egidy, and W. Wilhelm, Z. Phys. A **305**, 189 (1982).
[22] C. K. Hargrove, E. P. Hincks, G. R. Mason, R. J. McKee, D. Kessler, and S. Ricci, Phys. Rev. Lett. **23**, 215 (1969).
[23] K. P. Lohs, G. W. Wolschin, and J. Hüfner, Nucl. Phys. **A236**, 457 (1974).
[24] W. Y. Lee *et al*., Nucl. Phys. **A181**, 14 (1972).
[25] H. Backe *et al*., Nucl. Phys. **A234**, 469 (1974).
[26] A. Rüetschi, L. Schellenberg, T. Q. Phan, G. Piller, L. A. Schaller, and H. Schneuwly, Nucl. Phys. **A422**, 461 (1984).
[27] T. J. Stocki, D. F. Measday, E. Gete, M. A. Saliba, B. A. Moftah, and T. P. Gorringe, Nucl. Phys. **A697**, 55 (2002).
[28] NNDC at www.nndc.bnl.gov ENSDF files.

[29] R. G. Helmer and C. van der Leun, Nucl. Instrum. Methods A **450**, 35 (2000).
[30] M. S. Dewey, E. G. Kessler Jr., R. D. Deslattes, H. G. Börner, M. Jentschel, C. Doll, and P. Mutti, Phys. Rev. C **73**, 044303 (2006).
[31] S. Raman (private communication).
[32] Z. Revay (private communication).
[33] K. Shizuma, H. Inoue, and Y. Yoshizawa, Nucl. Instrum. Methods **137**, 599 (1976).
[34] Y. Lee, N. Hashimoto, H. Inoue, and Y. Yoshikawa, Appl. Radiat. Isotopes **43**, 1247 (1992).
[35] J. W. Kast, S. Bernow, S. C. Cheng, D. Hitlin, W. Y. Lee, E. R. Macagno, A. M. Rushton, and C. S. Wu, Nucl. Phys. **A169**, 62 (1971).
[36] T. Suzuki, D. F. Measday, and J. P. Roalsvig, Phys. Rev. C **35**, 2212 (1987).
[37] D. J. Abbott *et al*., Phys. Rev. A **55**, 214 (1997).
[38] M. J. Martin and P. H. Blichert-Toft, Nucl. Data Tables A **8**, 1 (1970).
[39] A. Wyttenbach, P. Baertschi, S. Bajo, J. Hadermann, K. Junker, S. Katcoff, E. A. Hermes, and H. S. Pruys, Nucl. Phys. **A294**, 278 (1978).
[40] B. MacDonald, J. A. Diaz, S. N. Kaplan, and R. V. Pyle, Phys. Rev. B **139**, 1253 (1965).
[41] M. Lifschitz, and P. Singer, Phys. Lett. **B215**, 607 (1988).
[42] Zhou Chunmei, Wang Gongqing, and Tao Zhenlan, Nucl. Data Sheets **83**, 145 (1998).
[43] D. Abbott *et al*., Phys. Rev. Lett. **80**, 5072 (1998).
[44] W. U. Schröder *et al*., Z. Phys. **268**, 57 (1974).
[45] G. Backenstoss, S. Charalambus, H. Daniel, Ch. von der Malsburg, G. Poelz, H. P. Povel, H. Schmitt, and L. Tauscher, Phys. Lett. **B31**, 233 (1970).
[46] G. Backenstoss, H. Daniel, H. Koch, Ch. von der Malsburg, G. Poelz, H. P. Povel, H. Schmitt, and L. Tauscher, Phys. Lett. **B43**, 539 (1973).
[47] H. K. Walter, Nucl. Phys. **A234**, 504 (1974).
[48] D. Branford *et al*., Phys. Rev. C **63**, 014310 (2000).
[49] B. Budick, R. Anigstein, and J. W. Kast, Nucl. Phys. **A350**, 265 (1980).
[50] B. Budick, R. Anigstein, and J. W. Kast, Phys. Lett. **B110**, 375 (1982).
[51] B. Budick, R. Anigstein, and J. W. Kast, Nucl. Phys. **A393**, 469 (1983).